**DOI:** 10.29298/rmcf.v14i76.1327

Research article

# ¿Mínimos cuadrados ordinarios o regresión frontera estocástica para estimar la línea de autoaclareo con la ecuación de *Yoda*?

# Ordinary least squares, or stochastic frontier regression to estimate the maximum density line with Yoda equation?

Juan Carlos Tamarit-Urias[1]*

Fecha de recepción/Reception date: 15 de diciembre de 2022.
Fecha de aceptación/Acceptance date: 24 de febrero de 2023

[1] Instituto Nacional de Investigaciones Forestales, Agrícolas y Pecuarias. Campo Experimental San Martinito. México.

*Autor para correspondencia; correo-e: tamarit.juan@inifap.gob.mx
*Corresponding author; e-mail: tamarit.juan@inifap.gob.mx

**Resumen**

La determinación precisa de la línea de autoaclareo mediante funciones tamaño-densidad junto con las guías para manejar la densidad (GMD) son insumos fundamentales para gestionar la densidad de rodales. Objetivos: (1) comparar las técnicas de ajuste de parámetros de mínimos cuadrados ordinarios lineales (MCO-L) combinada con criterios para desplazar la línea promedio y regresión frontera estocástica (RFE) para determinar la línea de autoaclareo con la ecuación de *Yoda*; (2) generar una GMD para *Pinus montezumae* en Puebla, México. Se utilizaron 90 sitios de muestreo circulares de 0.10 ha, ubicados en condición de alta densidad, cubrieron un amplio intervalo de edad y condiciones de crecimiento. Las variables número de árboles (*N*) y volumen promedio por árbol (*Vp*) se escalaron a una hectárea. Para MCO-L se aplicaron criterios teóricos para modificar el valor del intercepto (parámetro *α*) y desplazar la línea promedio a la frontera superior de las observaciones; para RFE se evaluaron las modalidades del modelo seminormal (MSN), modelo normal truncado (MNT) y modelo normal exponencial (MNE). Con el criterio de utilizar *Vp* y *N* del sitio con el índice de densidad del rodal máximo para aumentar el parámetro del intercepto, MCO-L reproduce una línea de autoaclareo similar a las modalidades de RFE. Por tanto, se seleccionó a RFE-MSN para reproducirla. El índice de densidad del rodal de *Yoda* fue de 9.2 $m^3$. Con una alometría específica y 100 árboles $ha^{-1}$ como densidad de referencia, se delimitaron las zonas de crecimiento de *Langsaeter* que conformaron la GMD, esta es útil para prescribir regímenes de aclareos.

**Palabras clave:** Aclareos, densidad del rodal, ley de -3/2, MCO o RFE, modelo tamaño-densidad, *Pinus montezumae* Lamb.

**Abstract**

Accurate determination of the self-thinning line using size-density functions together with density management guidelines (DMGs) are fundamental inputs for managing stand density. Objectives: (1) to compare linear ordinary least squares (OLS) parameter fitting techniques combined with criteria to shift the mean line and stochastic frontier regression (SFR) to determine the self-thinning line with the Yoda equation; (2) to generate a DMG for *Pinus montezumae* in *Puebla*, Mexico. Ninety circular 0.10 ha sampling sites were used, located in a high density condition, covering a wide range of ages and growth conditions. The variables number of trees (*N*) and average volume per tree (*aV*) were scaled to one hectare. For OLS, theoretical criteria were applied in order to modify the value of the intercept (parameter *a*) and move the average line to the upper boundary of the observations; for the SFR, the semi-normal model (SNM), the truncated normal model (TNM) and exponential normal model (ENM) modalities were evaluated. With the criterion of using the *aV* and *N* of the site with the maximum stand density index to increase the intercept parameter, the OLS, a self-thinning line similar to the SFR modes is reproduced. Therefore, SFR-SNM was selected to reproduce it. The density index of the Yoda stand was 9.2 m$^3$. With a specific allometry and 100 trees ha$^{-1}$ as reference density, Langsaeter's growth zones were delimited to form the DMG, which is useful for prescribing thinning regimes.

**Key words:** Thinnings, stand density, law of -3/2, OLS or SFR, size-density model, *Pinus montezumae* Lamb.

# Introduction

The values of the parameters (intercept and slope) of a self-thinning function are determined with different fitting methods and techniques, all oriented to improve the definition of the self-thinning line. Some of the main ones are: linear ordinary least squares, linear weighted ordinary least squares, reduced major axis, quantile regression, principal component analysis, mixed-effects model, segmented regression, hierarchical Bayesian model, and stochastic frontier regression (Solomon and Zhang, 2002; Zhang *et al.*, 2005; Sun *et al.*, 2010; Zhang *et al.*, 2015; Salas-Eljatib and Weiskittel, 2018; Aiguo *et al.*, 2019; Tian *et al*., 2021; Long *et al*., 2022).

The best of these techniques are linear ordinary least squares (OLS) and stochastic frontier regression (SFR); therefore, they are usually compared for the purpose of more accurately determining the self-thinning line for constructing density management guides (DMG) (Santiago-García *et al.*, 2013; Salas-Eljatib and

Weiskittel, 2018). However, in these contrasts, the theoretical criteria defined are not considered for linear ordinary least squares (OLS) in order to increase the value of the intercept and thus move the mean line to the upper boundary of the observations. From this perspective, in studies such as those by Camacho-Montoya *et al.* (2018), Quiñonez-Barraza *et al.* (2018), and Tamarit-Urias *et al.* (2019), it is evident that the OLS technique is at a clear disadvantage, which is why it is necessary to explore and compare this technique when the criteria referred to above are included.

The purpose of performing more objective tests is to define an accurate and efficient methodological process both for determining the self-thinning line and for constructing DMGs (Zhang *et al.*, 2005; VanderSchaaf and Burkhart, 2007; Salas-Eljatib and Weiskittel, 2018; Marchi, 2019; Tian *et al.*, 2021), in order to have alternative strategies with similar efficiency.

The self-thinning law or -3/2 was proposed by Yoda *et al.* (1963); it has biological, ecological, and mathematical foundations; it analyzes mortality due to extreme competition for space, nutrients, water, and sunlight in regular populations, with emphasis on monospecific even-aged stands (Weiskittel *et al*., 2011; Gavrikov, 2015; Lee and Choi, 2019). This mathematical relationship is given by the average weight of the population and its respective maximum number of living individuals that the site can support; it is defined by the ratio of the average plant volume (or biomass) to the number of individuals per surface area unit (Weller, 1987; Santiago-García *et al*., 2013; Xue *et al*., 2015).

The theoretical postulate of the Yoda function establishes that, for a given stand there is a maximum size-density relationship, which is independent of the age and quality site. When the logarithm of the average weight (volume or biomass) of the individuals is plotted against the logarithm of the number of trees, a straight line is obtained whose slope value is assumed to take a constant value of -1.5 (Yoda *et al.*, 1963). The main utility of the slope, along with the ordinate at the origin (intercept), is to determine the self-thinning line in response to high mortality due to extreme competition (Pretzsch, 2009; Schulze *et al.*, 2019; Long *et al*., 2022).

In population ecology, it has been accepted that the most important principle underlying stand density management is that of self-thinning, and that the self-thinning line determined with the Yoda function indicates the maximum possible density per surface area unit for a given species under a predetermined average volume per tree (Weller, 1987; Zeide, 1987; Gavrikov, 2015; Schulze *et al*., 2019). On the other hand, there is currently an ongoing international scientific debate as to whether the slope of the function is constant regardless of factors such as species, site quality, age and origin of the stand, geographic location, or other factors. In this sense, the validity of the value of a constant slope has been repeatedly questioned, and it has been documented to be significantly different in terms of species, site qualities, and management history (Weller, 1987; Zeide, 1987; Osawa and Allen, 1993; Solomon and Zhang, 2002; Fu *et al*., 2008; Ge *et al.*, 2017).
On the other hand, the guides or diagrams management density (GMD) of stands by prescribing thinning regimes are built upon the basis of the self-thinning line that reproduces size-density functions (Santiago-García *et al*., 2013; Brunet-Navarro *et al.*, 2016; Newton, 2021), among which the one proposed by Yoda stands out (Tian *et al.*, 2021).

DMGs are the main input and tool for managing the density of natural stands or commercial forest plantations (Tamarit-Urias *et al*., 2020; Newton, 2021). They provide an analytical foundation for the decisions to be made by the person responsible for forestry management on whether and to what extent to intervene in certain stands and thereby contribute to the improvement of the technical silvicultural management of forests.

*Pinus montezumae* Lamb. is a conifer with a broad distribution and is very abundant in the Transversal Neovolcanic Axis of Mexico. These trees reach heights of 25 to 30 m, and their wood is of high importance for its commercial use. They grows optimally at an average altitude of 2 500 m with 800 mm annual rainfall (Conafor, 2019). However, for this species there is a lack of a biologically and ecologically sound DMGs; therefore, according to Tamarit-Urias *et al*. (2020) and Newton (2021), it is necessary to develop this important tool to provide technical support for the evaluation of the levels of density and competition of the stands, as well as for the prescription of thinning, and thus contribute to the application of quantitative silviculture.

Two objectives were defined for these purposes: (1) to compare linear ordinary least squares parameter fitting techniques in combination with theoretical criteria to shift the mean line and stochastic frontier regression for the purpose of determining the self-thinning line with the Yoda equation; (2) to generate a DMG for natural stands of even-aged of *P. montezumae* in the state of *Puebla*, Mexico.

## Materials and Methods

The study was conducted in Forest Management Unit 2103, *Teziutlán* region, located in the northeastern part of *Puebla*, Mexico, between 20°02’34” and 19°36’34” N, and 97°43’46” and 97°22’23” W. The average altitude is 2 220 m, the average annual temperature fluctuates from 12 to 22 °C, and the soil type is Luvisol (Rodríguez-Acosta and Arteaga-Martínez, 2005).

The dasometric information was obtained from 90 circular sampling sites measuring 1 000 m$^2$, located in even-aged natural stands of *P. montezumae* under conditions of high density and competition. The criteria for establishing each sampling site were that *P.*

*montezumae* was the dominant species by at least 80 % in terms of the number of trees or the density within the stand, that no silvicultural interventions such as thinning and pruning had been carried out in the last five years prior to measurement, and that the phenomenon of crown closure was present. Thus, a wide range of age and growth conditions were covered. The dasometric variables generated per site were density expressed as the number of trees (*N*) and average tree volume (*aV*). The total volume of each tree for the species present at the sites was estimated with the allometric equations cited in Tamarit *et al.* (2022). The variables *N* and *aV* were scaled to the hectare level, and a database was formed to fit the Yoda size-density model (Yoda *et al*., 1963). Prior to the adjustment, the database was audited by graphical inspection to corroborate that the variables of interest showed biologically realistic behavior. Table 1 shows the basic statistics of the processed variables.

**Table 1.** Descriptive statistics of the dasometric variables analyzed and of some attributes of the stands *Pinus montezumae* Lamb.

| Variable | Minimum | Mean | Maximum | *SD* | *CV* |
|---|---|---|---|---|---|
| *N* (trees ha$^{-1}$) | 190.00 | 910.00 | 3 390.00 | 740.3901 | 81.3616 |
| *aV* (average volume, m$^3$) | 0.0802 | 0.8649 | 2.8855 | 0.7908 | 91.4311 |
| Quadratic mean diameter (cm) | 11.5060 | 25.2581 | 45.9213 | 10.2030 | 40.3951 |
| Basal area (m$^2$ ha$^{-1}$) | 14.6153 | 30.4573 | 48.7698 | 7.7230 | 25.3567 |
| Volume (m$^3$ ha$^{-1}$) | 148.89 | 407.11 | 836.79 | 149.70 | 36.77 |
| Age (years) | 13.00 | 35.80 | 104.00 | 20.95 | 58.50 |

*SD* = Standard deviation; *CV* = Coefficient of variation as a percentage.

The parameters of the Yoda function in linear form were estimated with the linear ordinary least squares (OLS) technique; their mathematical structure was represented by Equation (1).

$$ln(aV) = ln(\alpha) + \beta\ ln(N) + \varepsilon \qquad (1)$$

Where:

$ln$ = Natural logarithm function

$\alpha$ and $\beta$ = Parameters for estimation

*N* = Number of trees

$\varepsilon$ = Term of the error *[$\varepsilon$=iid N(0, $\sigma^2$)]*

*iid* = Indicates that the error is independent and identically distributed

When the function parameters were estimated with the stochastic frontier regression (SFR) technique, the structure was represented by Equation (2).

$$ln(aV) = ln(\alpha) + \beta\ ln(N) - u + v \qquad (2)$$

Where the error is divided as follows: (1) $u_i$ is an asymmetric term corresponding to an error component that accounts for technical inefficiency in the observed data and is assumed to be distributed independently of $v_i$ and regressors; (2) $v_i$ is a component of the error associated with the measurement of individual observations; it is assumed to be a symmetrical disturbance distributed independently of $u_i$, incorporating the random variations due to factors such as random errors, observation errors and data measurement errors, are distributed as follows $v$=*iid*

*N(0, $\sigma^2_v$)* (Bi, 2004; Comeau *et al*., 2010; Salas-Eljatib and Weiskittel, 2018; Tian *et al.*, 2021; Long *et al.*, 2022).

Based on these assumptions, statistical distributions that tend to be one-sided, such as the SFR modalities: semi-normal model (SNM) and exponential normal model (ENM), are selected for $u_i$. When the value of the technical inefficiency $u_i$ is assumed to be zero, then the model *iid N+(0, $\sigma^2_u$)* corresponds to the SNM; if the $u_i$ (*i*=1..., *N*) are non-negative random variables, then *iid N+(0, $\sigma^2_u$)* is defined as the truncated-normal model in zero (TNM) (Bi, 2004; Zhang *et al.*, 2013; Tian *et al.*, 2021). For parameter estimation with SFR, the SNM, TNM and ENM modalities were evaluated.

The adjustment of the Yoda equation with OLS was carried out with the R software (R Core Team, 2022), version 4.2. In order to fit the same function with the SFR technique using maximum likelihood, the Frontier package of the R software was utilized.

After the OLS adjustment, four basic theoretical criteria with a statistical basis were applied to increase the value of the intercept (parameter $\alpha$) cited in Coma *et al.* (2010), Burkhart and Tomé (2012), and Tamarit-Urias *et al.* (2020), and adapted for the Yoda function. Thus, the value of the slope parameter ($\beta$) was kept fixed, and, with the increased values of the intercept ($\alpha_{max}$), the average line was shifted towards the upper limit of the observed values in order to obtain the maximum density lines. The expressions that estimated the values of $\alpha_{max}$ for each criterion were:

Criterion A: $\alpha_{max} = (1.96 * \sigma^2) + \alpha$ (3)

Criterion B: $\alpha_{max} = ln(Vp_{+}) + \beta * ln(N_{+})$ (4)

Criterion C: $\alpha_{max} = \bar{x}_{3RM} + \alpha$ (5)

Criterion D: $\alpha_{max} = ULCI$ (6)

Where:

$\sigma^2$ = Variance of error

$Vp_+$ and $N_+$ = Average volume per tree and density values for the site with the highest Yoda Stand Density Index

$\bar{x}_{3RM}$ = Average of the three major residuals

$ULCI$ = Value of the upper limit of the confidence interval for the parameter $\alpha$ calculated at 95 % confidence.

In the first stage, the OLS methodology analyzed the significance of the parameters, the standard errors and the variance of the error. In the SFR methodology, based on Santiago-García *et al.* (2013) and Quiñonez-Barraza *et al.* (2018), the quality of fit between the SNM, TNM and ENM modalities was compared by means of the log likelihood (*logLik*), the Akaike information criterion (*AIC*) and the Schwarz criterion (*SchC*), as well as of the error component variances ($\sigma^2_v$ and $\sigma^2_u$), the ratio of error component variances ($\lambda$), and the total variance ($\sigma^2$) (Bi, 2004; Comeau *et al*., 2010). The significance of the parameters was also examined.

In a second phase, a comparative graphical analysis based on Salas-Eljatib and Weiskittel (2018) was carried out between the self-thinning lines generated by each of the techniques (between criteria for increasing $\alpha$ with OLS and between the fitting modalities with SFR). In addition, the location and trajectories of the self-thinning lines were inspected and contrasted with the observed data.

In the selection of the best fit technique, a balance between statistical criteria (conceptual theoretical framework and goodness-of-fit statistics) and biological reasons for growth was favored.

With the values of the parameters of the best fit technique, the self-thinning line was delimited for *P. montezumae* in the study area, which corresponds to the largest average volume per tree that a hectare can support without self-thinning and is equivalent to 100 % of the Yoda stand density index (*YSDI*) (Santiago-García *et al.*, 2013). A reference density (*Nr*) of 100 trees ha$^{-1}$ was determined in order to calculate the *YSDI*. The *YSDI* is estimated by algebraically manipulating the linearized Yoda equation and applying the exponential function ($e$) as the inverse of the natural logarithm; the nonlinear mathematical structure of this index is represented by the expression (7).

$$YSDI = aV\ (Nr/N)^{-\beta} \qquad (7)$$

The maximum *YSDI* ($YSDI_{max}$) was estimated using the expression (8).

$$YSDI_{max} = e^{(\alpha - \beta\ ln(Nr))} \qquad (8)$$

Where the components of both expressions were previously indicated.

The DMG was constructed considering as reference the self-thinning line to determine the four Langsaeter's (1941) growth zones that form bands of relative densities and correspond to particular stages of stand development (Pretzsch, 2009). These areas were obtained by means of theoretical lines that correspond to percentages of the $YSDI_{max}$. According to Tamarit-Urias *et al.* (2020), zone 1 of site underutilization corresponded to 25 %; zone 2, which is transition zone, was defined as 25 to 35 %; area 3 of maximum growth in volume per hectare, was located between 35 and 70 %, and area 4, corresponding to self-thinning, was located in the range of 70 to 100 %.

The value of the slope parameter ($\beta$) obtained with the selected fitting technique was contrasted with the constant theoretical value of -1.5 established by Yoda *et al.* (1963) using the likelihood ratio and Wald tests (Santiago-García *et al*., 2013; Aiguo *et al*., 2019), was also compared with values recorded for other taxa.

## Results and Discussion

Table 2 shows the statistical adjustment of the Yoda function by OLS and by SFR in the three evaluated modalities. All parameters and error components, except $\sigma^2_u$ for SFR-TNM, were significant ($p$<0.05), the values of the standard errors were low. Table 3 shows the values of the goodness-of-fit statistics, both for OLS and for the modalities of the SFR technique; the best values for total variance, variance ratio, *AIC*, and *SchC* were presented by SFR-SNM; the *logLik* value for this modality was the second best, it also exhibited the lowest standard error values for the parameters $\alpha$ and $\beta$. For its part, the error variance with the OLS technique was 0.32703.

**Table 2.** Parameter values and goodness-of-fit statistics obtained by the linear ordinary least squares (OLS) and stochastic frontier regression (SFR) approaches.

| Fitting technique | Parameter | Estimator | Standard error | *t*-value | Significance |
|---|---|---|---|---|---|
| OLS | $\alpha$ | 7.555390 | 0.307560 | 24.57 | <0.0001 |
| | $\beta$ | -1.246920 | 0.046780 | -26.66 | <0.0001 |
| SFR-SNM | $\alpha$ | 8.051316 | 0.258740 | 31.12 | <0.0001 |
| | $\beta$ | -1.264345 | 0.036818 | -34.34 | <0.0001 |
| | $\sigma^2_v$ | 0.142798 | 0.041478 | 3.44 | 0.0006 |
| | $\sigma^2_u$ | 0.479931 | 0.064110 | 7.49 | <0.0001 |
| SFR-TNM | $\alpha$ | 8.004173 | 0.315643 | 25.36 | <0.0001 |
| | $\beta$ | -1.261065 | 0.038616 | -32.66 | <0.0001 |
| | $\sigma^2_v$ | 0.153761 | 0.058794 | 2.62 | 0.0089 |
| | $\sigma^2_u$ | 0.533216 | 0.278571 | 1.91 | 0.0556 |
| SFR-ENM | $\alpha$ | 7.580781 | 0.398343 | 19.03 | <0.0001 |
| | $\beta$ | -1.201906 | 0.060889 | -19.74 | <0.0001 |
| | $\sigma^2_v$ | 0.358133 | 0.089226 | 4.01 | <0.0001 |
| | $\sigma^2_u$ | 0.245084 | 0.072550 | 3.38 | 0.0007 |

**Table 3.** Goodness-of fit statistics for linear ordinary least squares (OLS-L) and stochastic frontier regression modes (SFR).

| Fitting technique | *logLik* | *AIC* | *SchC* | $\sigma^2$ | $\lambda$ |
|---|---|---|---|---|---|
| OLS * | -26.09852 | 58.19704 | 65.69647 | 0.32703 | - |
| SFR-SNM | -21.43774 | 50.87549 | 60.87473 | 0.50072 | 3.36090 |
| SFR-TNM | -21.40915 | 52.81829 | 65.31734 | 0.55494 | 3.46783 |
| SFR-ENM | -33.25753 | 74.51506 | 84.51430 | 0.43396 | 0.68434 |

*logLik* = Logarithm of likelihood; *AIC* = Akaike information criterion; *SchC* = Schwarz criterion; $\sigma^2$ = Total error variance; $\lambda$ = Variance ratio ($\sigma^2_u/\sigma^2_v$). *The values of the coefficient of determination ($R^2$) and of the root mean square of the error (*RMSE*) are 0.8898 and 0.3234 m$^3$, respectively.

Figure 1a shows the graphical behavior of the maximum density lines generated by the OLS technique combined with the theoretical criteria for shifting the average line, whose calculated values for $\alpha_{max}$ were 8.19637, 8.01095, 7.97680, and 8.16660, for criteria A, B, C, and D, respectively. Whereas Figure 1b shows the self-thinning lines produced by the SFR technique in SNM, TNM, and ENM modes.

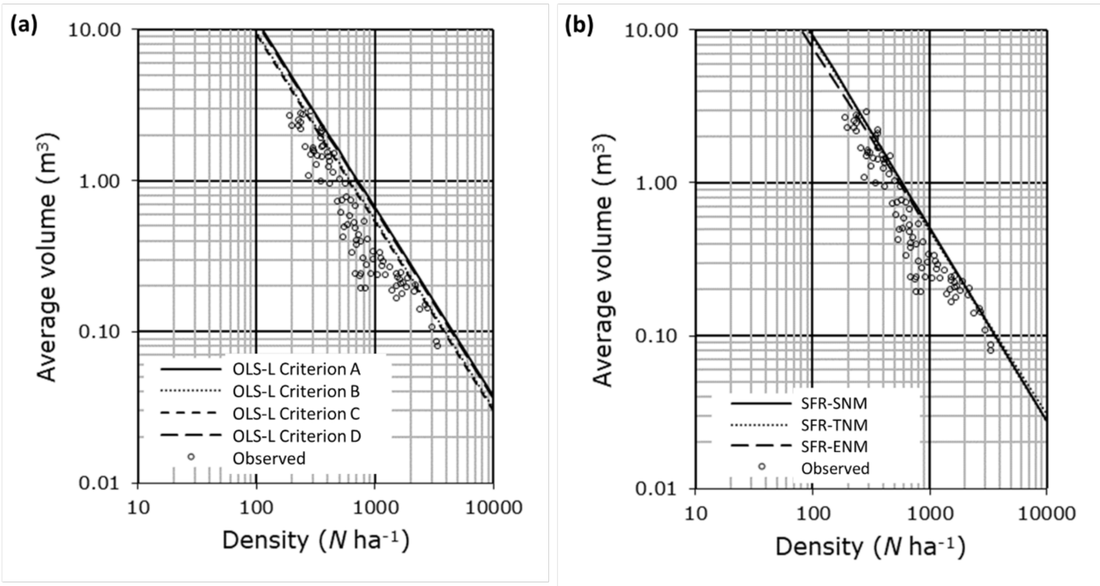


**Figure 1.** Self-thinning lines obtained by OLS (a) and SFR (b) techniques with respect to observed data.

With both fitting techniques and their modalities, it was observed that all the self-thinning lines are located at the upper limit of the observed data, so they can be considered as biological lines of maximum density *per se* (Figure 1). A more detailed visual analysis shows that the OLS technique in combination with the theoretical criterion B is more consistent and biologically reasonable compared to the rest of the criteria, because the maximum density line is better positioned at the upper limit (Figure 1a). Methodologically, this criterion is robust since the modification of the intercept is based on the site with the *YSDI* having the highest value (with *Nr*=100 trees ha$^{-1}$ and $\beta$=-1.24692); a situation that makes the self-thinning line intercept the point *aV-N* corresponding to the site with the highest *YSDI*, whereby $YSDI/YSDI_{max}=1$.

The SFR technique reproduces maximum density lines that correspond to absolute maxima, so they are automatically located at the upper boundary. A visual comparative analysis of the SFR lines showed that the SNM modality has a superior pattern because the line was better positioned at the upper limit of the boundary of the observations (Figure 1b).

The graphical comparison of the two techniques for estimating the fitting parameters (OLS with criterion B and SFR-SNM) showed that they are similar and close to each other (Figure 2a), because both are acceptably located at the upper limit of the observed data. The OLS line lies slightly on the outermost part of the observations because it has a lower slope ($\beta$=-1.24692 for OLS *vs* $\beta$=-1.264345 for SFR-SNM), and a lower intercept ($\alpha_{max}$=8.010952 for OLS *vs* $\alpha$=8.051316 for SFR-SNM).

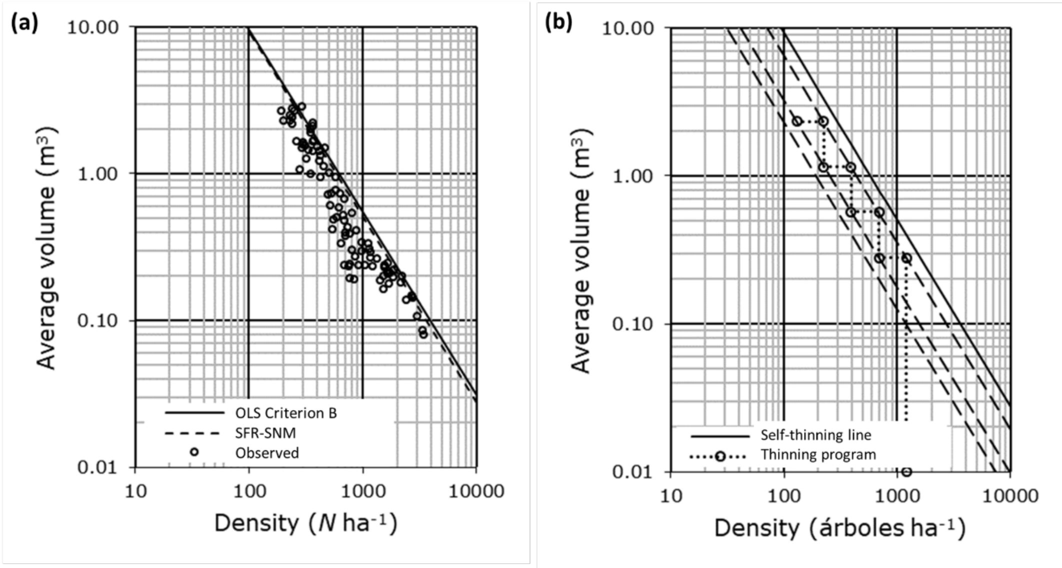


**Figure 2.** Comparison between self-thinning lines obtained by OLS-Criterion B and SFR-SNM (a), DMG constructed for *Pinus montezumae* Lamb. with the Yoda function fitted by SFR-SNM and prescription of a thinning program (b).

Given this similarity, SFR-SNM was chosen because this technique has a robust theoretical framework (Tian *et al.*, 2021; Long *et al.*, 2022) and has the additional advantage of allowing direct, immediate determination of the self-thinning line. In this regard, Bi (2004) cites that SFR estimates extreme or "frontier" values of the analyzed data set; Comeau *et al.* (2010) add that, as a stochastic process, the frontier itself is considered to be a random variable in which each experimental data has its own frontier function, which is different from the general function. The immediate effect of using it in certain size-density functions, such as Yoda's, is that it automatically improves the objective determination of the self-thinning line. Therefore, according to Zhang *et al.* (2005), Kimsey *et al*. (2019), and Tian *et al.* (2021), it could be inferred that SFR is comparatively more straightforward, efficient, and consistent.

In Mexico, the parameter estimation technique using SFR in the SNM modality has been satisfactorily utilized by Santiago-García *et al.* (2013) in order to delimit the self-thinning line with Yoda's index for *Pinus patula* Schltdl. & Cham.

However, the graphical results of the self-thinning line estimated with OLS indicate that this is also an effective technique. In this sense, it is considered that further studies could use OLS in combination with the theoretical criteria to shift the average line. Thus, this type of exploratory analysis for other taxa, with an emphasis on the graphical behavior of the self-thinning lines they reproduce, will make it possible to determine the combination that best represents the observed data. The OLS technique is robust and objective for estimating the mean condition because it minimizes the sum of squares of the errors (Zhang *et al.*, 2005; Comeau *et al.*, 2010). In addition, Long *et al*. (2022) point out that traditional methods for estimating the self-thinning line, such as criterion B, which utilizes the $YSDI_{max}$ and, implicitly, the relative density method, are based on stand-growth dynamics and incorporate important biological criteria, aspects that are omitted by the SFR technique.

The DMG for *P. montezumae* stands was constructed with the SFR-SNM adjustment (Figure 2b). The *YSDI* of the free-growth line (25 %) was estimated at 2.3 $m^3$, the *YSDI* for the constant-growth line (35 %) was 3.2 $m^3$, for the mortality onset line (70 %) the *YSDI* was 6.5 $m^3$, and for the self-thinning line (100 %) it was 9.2 $m^3$, which corresponds to the $YSDI_{max}$.

The use of the DMG is exemplified by assuming a hypothetical stand with an initial density of 1 200 trees $ha^{-1}$; based on this condition, a theoretical systematic thinning program is generated in which the stand density must be managed in the growth zone 3 (Figure 2B). DMG has a broad utility in achieving various production objectives, as it makes it possible to derive multiple thinning scenarios and select the most convenient one to plan density management strategies.

Based on the likelihood ratio and Wald tests (with $\alpha$=0.05), it was determined that the slope value of -1.264345, by SFR-SNM, is statistically different from the constant theoretical value of -1.5 ($P$<0.0001) proposed by Yoda *et al.* (1963); the 95 % confidence interval for $\beta$ ranged from -1.3428 to -1.1674 and did not include -1.5. This result is consistent with the one registered by Santiago-García *et al.* (2013), who, using the same fitting technique and modality for *P. patula* stands in *Hidalgo*, Mexico, estimated a value of -1.1999 for $\beta$; as in the previous case, the respective interval did not include -1.5.

Other studies for different forest species in different ecoregions of Mexico and the world also cite values that are different from -1.5 (Table 4). In certain cases, it has been observed that the slope coefficients are significantly lower than the theoretical value, suggesting that forest stands of these species grow at higher rates because they are located on sites with a higher productive capacity.

**Table 4.** Comparison of the value of the slope parameter ($\beta$) of the Yoda equation for *Pinus montezumae* Lamb. with respect to other species.

| Species | Locality/country | $\beta$ value | Documentary reference |
|---|---|---|---|
| *Pinus montezumae* Lamb. | *Teziutlán*, *Puebla*, Mexico | -1.264345 | Present study |
| *Pinus patula* Schltdl. & Cham. | *Zacualtipán*, *Hidalgo*, Mexico | -1.199907 | Santiago-García *et al*. (2013) |
| *Pinus halepensis* Mill. | Catalonia, Spain | -1.77700 | Brunet-Navarro *et al*. (2016) |
| *Pinus nigra* J. F. Arnold | Catalonia, Spain | -1.78700 | Brunet-Navarro *et al*. (2016) |
| *Pinus sylvestris* L. | Catalonia, Spain | -1.64700 | Brunet-Navarro *et al*. (2016) |
| *Pinus uncinata* Raymond ex A. DC. | Catalonia, Spain | -1.66500 | Brunet-Navarro *et al*. (2016) |
| *Picea mariana* (Mill.) Britton, Sterns & Poggenb. | Newfoundland, Canada | -1.618000 | Newton y Weetman (1993) |
| *Abies balsamea* (L.) Mill. | New Brunswick, Canada | -1.339954 | Penner *et al*. (2006) |
| *Abies balsamea* (L.) Mill. | Newfoundland, Canada | -1.282000 | McCarthy y Weetman (2007) |
| *Abies balsamea* (L.) Mill. | New Brunswick, Canada | -1.403980 | Swift *et al*. (2007) |
| *Cunninghamia lanceolata* (Lamb.) Hook. | Fujian, China | -1.470000 | Zhang *et al*. (2015) |
| *Larix decidua* Mill. | Maine, USA | -1.774000 | Gilmore y Briggs (2003) |
| *Kandelia obovata* Sheue, H. Y. Liu & J. Yong | Okinawa, Japan | -1.585000 | Kamara *et al*. (2012) |

Within this context, the evidence leads to reaffirm the argument that the value of $\beta$ is not always close to the theoretical value and may differ significantly between species (Comeau *et al.*, 2010; Santiago-García *et al.*, 2013; Brunet-Navarro *et al.*, 2016), this behavior is partly explained by the fact that different populations have different mortality rates depending on their density, growth habits, shade tolerance, site productivity factors and stand age (Weller, 1987; Bi, 2004). Other factors that may cause $\beta$ to differ from -3/2 are the species, the sample size and the manner of sample selection, the equations used to estimate tree volume, the technique and regression algorithm implemented, and whether the processed data set do indeed come from stands that represent the maximum size-density combination for the phenomenon of self-thinning to occur (Puntiere, 1993; Bi, 2004; McCarthy and Weetman, 2007). The above ratifies the postulate that a specific allometry should be developed for each species of interest and ecoregion in order to avoid errors when estimating and controlling density (Osawa and Allen, 1993; Tamarit-Urias *et al*., 2020; Long *et al*., 2022).

## Conclusions

The present study made it clear that the self-thinning line with the Yoda equation for *Pinus montezumae* stands in *Puebla*, Mexico, can be determined as an absolute biological maximum and, with more efficient statistical properties, by using the stochastic frontier regression technique in its semi-normal model modality. Similar effects are also obtained when the linear ordinary least squares technique is combined with the theoretical criteria to increase the value of the intercept and thus shift the mean line. In particular, the criterion based on the site with the highest value of *YSDI* produces very similar effects to that of SFR-SNM. The self-thinning line and the maximum stand density index were determined on a point basis; both attributes are fundamental to evaluate the level of density and competition of stands.

The DMG thus constructed is an important silvicultural tool, specific to this taxon in a particular ecoregion; the DMG together with the density parameters referred to are biologically based and scientifically supported. The value of the slope parameter of the Yoda equation for the species studied was statistically different from the theoretical value of -1.5; the comparison of this value between different species demonstrated and ratified the postulate that it varies significantly between taxa with respect to the theoretical value; therefore, the premise is reaffirmed that studies aimed at assessing competition, defining the maximum density line, and constructing density guides must be carried out with a specific and independent allometry.

## Acknowledgments

The author is grateful to the anonymous reviewers who contributed to the improvement of this final version.

## Conflict of interest

The author declares that he did not participate in the editorial process of the manuscript.

## Contribution by author

Juan Carlos Tamarit-Urias: conceptualization and organization of the research, database building, statistical analysis, writing and proofreading of the paper.

# References

Aiguo, D., F. Lihua and Z. Jianguo. 2019. Self-thinning rules at Chinese fir (*Cunninghamia lanceolata*) plantations—based on a permanent density trial in southern China. Journal of Resources and Ecology 10(3):315-323. Doi: 10.5814/j.issn.1674-764x.2019.03.010.

Bi, H. 2004. Stochastic frontier analysis of a classic self-thinning experiment. Austral Ecology A Journal of ecology in the Southern Hemisphere 29(4):408-417. Doi: 10.1111/j.1442-9993.2004.01379.x.

Brunet-Navarro, P., F. J. Sterck, J. Vayreda, J. Martinez-Vilalta and G. M. J. Mohren. 2016. Self-thinning in four pine species: an evaluation of potential climate impacts. Annals of Forest Science 73(4):1025-1034. Doi: 10.1007/s13595-016-0585-y.

Burkhart, H. E. and M. Tomé. 2012. Modeling forest trees and stands. Springer. New York, NY, United States of America. 458 p.

Camacho-Montoya, J. A., W. Santiago-García, G. Rodríguez-Ortiz, P. Antúnez, E. Santiago-García y M. E. Suárez-Mota. 2018. Autoaclareo y manejo de la densidad en rodales coetáneos de *Pinus patula* Schiede ex Schlechtdl. & Cham. Revista Mexicana de Ciencias Forestales 9(49):188-212. Doi: 10.29298/rmcf.v9i49.162.

Comeau, P. G., M. White, G. Kerr and S. E. Hale. 2010. Maximum density-size relationships for Sitka spruce and coastal Douglas-fir in Britain and Canada.

Forestry: An International Journal of Forest Research 83(5):461-468. Doi: 10.1093/forestry/cpq028.

Comisión Nacional Forestal (Conafor). 2019. Paquetes Tecnológicos *Pinus montezumae* *Lamb.* http://www.conafor.gob.mx:8080/documentos/docs/13/971Pinus%20montezumae.pdf. (25 de noviembre de 2022).

Fu, L. H., J. G. Zhang, A. G. Duan, H. G. Sun and C. Y. He. 2008. Review of studies on maximum size-density rules. Chinese Journal of Plant Ecology 32(2):501-511. Doi: 10.3773/j.issn.1005-264x.2008.02.030.

Gavrikov, V. L. 2015. An application of bole surface growth model: a transitional status of '−3/2' rule. European Journal of Forest Research 134(4):715-724. Doi: 10.1007/s10342-015-0885-z.

Ge, F., W. Zeng, W. Ma and J. Meng. 2017. Does the slope of the self-thinning line remain a constant value across different site qualities? -An implication for plantation density management. Forests 8(10):355-367. Doi: 10.3390/f8100355.

Gilmore, D. W. and R. D. Briggs. 2003. A stocking guide for European larch in eastern North America. Northern Journal of Applied Forestry 20(1):34-38. Doi: 10.1093/njaf/20.1.34.

Kamara, M., R. Deshar, S. Sharma, Md. Kamruzzaman and A. Hagihara. 2012. The self-thinning exponent in overcrowded stands of the mangrove, *Kandelia obovata*, on Okinawa Island, Japan. Journal of Oceanography 68(6):851-856. Doi: 10.1007/s10872-012-0135-7.

Kimsey Jr., M. J., T. M. Shaw and M. D. Coleman. 2019. Site sensitive maximum stand density index models for mixed conifer stands across the Inland Northwest, USA. Forest Ecology and Management 433:396-404. Doi: 10.1016/j.foreco.2018.11.013.

Langsaeter, A. 1941. Om tynning i enaldret gran-og furuskog. Meddelelser fra Det norske skogforsøksvesen 8:13-216. https://nibio.brage.unit.no/nibio-xmlui/handle/11250/2988571?show=full. (4 de noviembre de 2022).

Lee, D. and J. Choi. 2019. Evaluating maximum stand density and size–density relationships based on the competition density rule in Korean pines and Japanese larch. Forest Ecology and Management 446:204-213. Doi: 10.1016/j.foreco.2019.05.017.

Long, S., S. Zeng, Z. Shi and S. Yang. 2022. Estimating the self-thinning boundary line for oak mixed forests in central China by using stochastic frontier analysis and a proposed variable density model. Ecology and Evolution 12(9):e9064. Doi: 10.1002/ece3.9064.

Marchi, M. 2019. Nonlinear versus linearised model on stand density model fitting and stand density index calculation: analysis of coefficients estimation via simulation. Journal of Forestry Research 30(5):1595-1602. Doi: 10.1007/s11676-019-00967-0.

McCarthy, J. W. and G. Weetman. 2007. Self-thinning dynamics in a balsam fir (*Abies balsamea* (L.) Mill.) insect-mediated boreal forest chronosequence. Forest Ecology and Management 241(1-3):295-309. Doi: 10.1016/j.foreco.2007.01.001.

Newton, P. F. and G. F. Weetman. 1993. Stand density management diagrams and their development and utility in black spruce management. The Forestry Chronicle 69(4):421-430. Doi: 10.5558/tfc69421-4.

Newton, P. F. 2021. Croplanner: A stand density management decision-support software suite for addressing volumetric yield, end-product and ecosystem service objectives when managing boreal conifers. Forests 12(4):448. Doi: 10.3390/f12040448.

Osawa, A. and R. B. Allen. 1993. Allometric theory explains self-thinning relationships of mountain beech and red pine. Ecology 74(4):1020-1032. Doi: 10.2307/1940472.

Penner, M., D. E. Swift, R. Gagnon and J. Brissette. 2006. A stand density management diagram for balsam fir in New Brunswick. The Forestry Chronicle 82(5):700-711. Doi: 10.5558/tfc82700-5.

Pretzsch, H. 2009. Forest dynamics, growth and yield. From measurement to model. Springer-Verlag Berlin. Heidelberg, BW, Germany. 664 p.

Puntieri, J. G. 1993. The self-thinning rule: bibliography revision. Preslia Praha 65(3):243-267. https://www.preslia.cz/article/pdf?id=11447. (11 noviembre de 2022).

Quiñonez-Barraza, G., J. C. Tamarit-Urias, M. Martínez-Salvador, X. García-Cuevas, H. M. De los Santos-Posadas and W. Santiago-García. 2018. Maximum density and density management diagram for mixed-species forests in Durango, Mexico. Revista Chapingo Serie Ciencias Forestales y del Ambiente 24(1):73-90. Doi: 10.5154/r.rchscfa.2017.09.056.

R Core Team. 2022. The R Project for Statistical Computing (Version 4.2.3). Vienna, Austria. R Foundation for Statistical Computing. https://www.r-project.org/. (11 de noviembre de 2022).

Rodríguez-Acosta, M. y B. Arteaga-Martínez. 2005. Índice de sitio para *Pinus chiapensis* (Martínez) Andresen, en los estados de Veracruz y Puebla, México. Revista Chapingo Serie Ciencias Forestales y del Ambiente 11(1):39-44. https://www.redalyc.org/pdf/629/62911106.pdf. (18 noviembre de 2022).

Salas-Eljatib, C. and A. R. Weiskittel. 2018. Evaluation of modeling strategies for assessing self-thinning behavior and carrying capacity. Ecology and Evolution 8(22):10768-10779. Doi: 10.1002/ece3.4525.

Santiago-García, W., H. M. De los Santos-Posadas, G. Ángeles-Pérez, J. R. Valdez-Lazalde, D. H. Del Valle-Paniagua y J. J. Corral-Rivas. 2013. Auto-aclareo y guías de densidad para *Pinus patula* mediante el enfoque de regresión de frontera estocástica. Agrociencia 47(1):75-89. http://www.scielo.org.mx/pdf/agro/v47n1/v47n1a7.pdf. (29 de julio de 2022).

Schulze, E. D., E. Beck, N. Buchmann, S. Clemens, K. Müller-Hohenstein and M. Scherer-Lorenzen. 2019. Plant ecology. Springer-Verlag Berlin. Heidelberg, BW, Germany. 926 p.

Solomon, D. S. and L. Zhang. 2002. Maximum size-density relationships for mixed softwoods in the northeastern USA. Forest Ecology and Management 155(1-3):163-170. Doi: 10.1016/S0378-1127(01)00556-4.

Sun, H. G., J. G. Zhang and A. G. Duan. 2010. A comparison of selecting data points and fitting coefficients methods for estimating self-thinning boundary line. Chinese Journal of Plant Ecology 34(4):409-417. Doi: 10.3773/j.issn.1005-264x.2010.04.006.

Swift, E., M. Penner, R. Gagnon and J. Knox. 2007. A stand density management diagram for spruce–balsam fir mixtures in New Brunswick. The Forestry Chronicle 83(2):187-197. Doi: 10.5558/tfc83187-2.

Tamarit-Urias, J. C., G. Quiñonez-Barraza, H. M. De los Santos-Posadas, A. Castañeda-Mendoza and W. Santiago-García. 2019. A stand density diagram for *Pinus patula* Schiede ex Schltdl. & Cham. in Puebla, Mexico. Revista Mexicana de Ciencias Forestales 10(51):157-181. Doi: 10.29298/rmcf.v10i51.223.

Tamarit-Urias, J. C., G. Quiñonez-Barraza y J. Hernández-Ramos. 2020. Aspectos metodológicos para generar diagramas de manejo de la densidad de rodales con base en el índice de Reineke. Revista Mexicana de Ciencias Forestales 11(61):4-26. Doi: 10.29298/rmcf.v11i61.728.

Tamarit U., J. C., M. Rodríguez A. e I. Lerma S. 2022. SIIMADER: Sistema informático Inifap para manejar la densidad de rodales. e-Cucba 9(17):147-155. Doi: 10.32870/ecucba.vi17.223.

Tian, D., H. Bi, X. Jin and F. Li. 2021. Stochastic frontiers or regression quantiles for estimating the self-thinning surface in higher dimensions? Journal of Forestry Research 32:1515-1533. Doi: 10.1007/s11676-020-01196-6.

VanderSchaaf, C. L. and H. E. Burkhart. 2007. Comparison of methods to estimate Reineke's maximum size-density relationship species boundary line slope. Forest Science 53(3):435-442. Doi: 10.1093/forestscience/53.3.435.

Weiskittel, A. R., D. W. Hann, J. A. Kershaw and J. K. Vanclay. 2011. Forest growth and yield modeling. Jhon Wiley & Sons. Ltd. Chichester, WS, United Kingdom. 415 p.

Weller, D. E. 1987. A reevaluation of the -3/2 power rule of plant self-thinning. Ecological Monographs 57(1):23-43. Doi: 10.2307/1942637.

Xue, L., X. Hou, Q. Li and Y. Hao. 2015. Self-thinning lines and allometric relation in Chinese fir (*Cunninghamia lanceolata*) stands. Journal of Forestry Research 26(2):281-290. Doi: 10.1007/s11676-015-0059-3.

Yoda, K., T. Kira, H. Ogawa and K. Hozumi. 1963. Self-thinning in overcrowded pure stands under cultivated and natural conditions (Intraspecific competition among higher plants. XI). Journal of Biology 14:107-129. https://refhub.elsevier.com/S0378-1127(21)01097-5/h0445. (29 de julio de 2022).

Zeide, B. 1987. Analysis of the 3/2 power law of self-thinning. Forest Science 33(2):517-537. Doi: 10.1093/forestscience/33.2.517.

Zhang, L., H. Bi, J. H. Gove and L. S. Heath. 2005. A comparison of alternative methods for estimating the self-thinning boundary line. Canadian Journal of Forest Research 35:1507-1514. Doi: 10.1139/x05-070.

Zhang, J., W. W. Oliver and R. F. Powers. 2013. Reevaluating the self-thinning boundary line for ponderosa pine (*Pinus ponderosa*) forests. Canadian Journal of Forest Research 43(10):963-971. Doi: 10.1139/cjfr-2013-0133.

Zhang, X., J. Zhang and A. Duan. 2015. A hierarchical bayesian model to predict self-thinning line for chinese fir in southern China. Plos One 10(10):e0139788. Doi: 10.1371/journal.pone.0139788.

Todos los textos publicados por la **Revista Mexicana de Ciencias Forestales –**sin excepción– se distribuyen amparados bajo la licencia *Creative Commons 4.0* Atribución-No Comercial (CC BY-NC 4.0 Internacional), que permite a terceros utilizar lo publicado siempre que mencionen la autoría del trabajo y a la primera publicación en esta revista.